UCRL-JC-132511
Preprint

Stress Corrosion Cracking of Ni-Base and Ti Alloys Under Controlled Potential

Ajit K. Roy
John C. Estill
Steven R. Gordon
Lawrence F. Logoteta

This paper was prepared for submittal to
Seventh International Conference on Nuclear Engineering
Tokyo, Japan
April 19-23, 1999

October 22, 1998

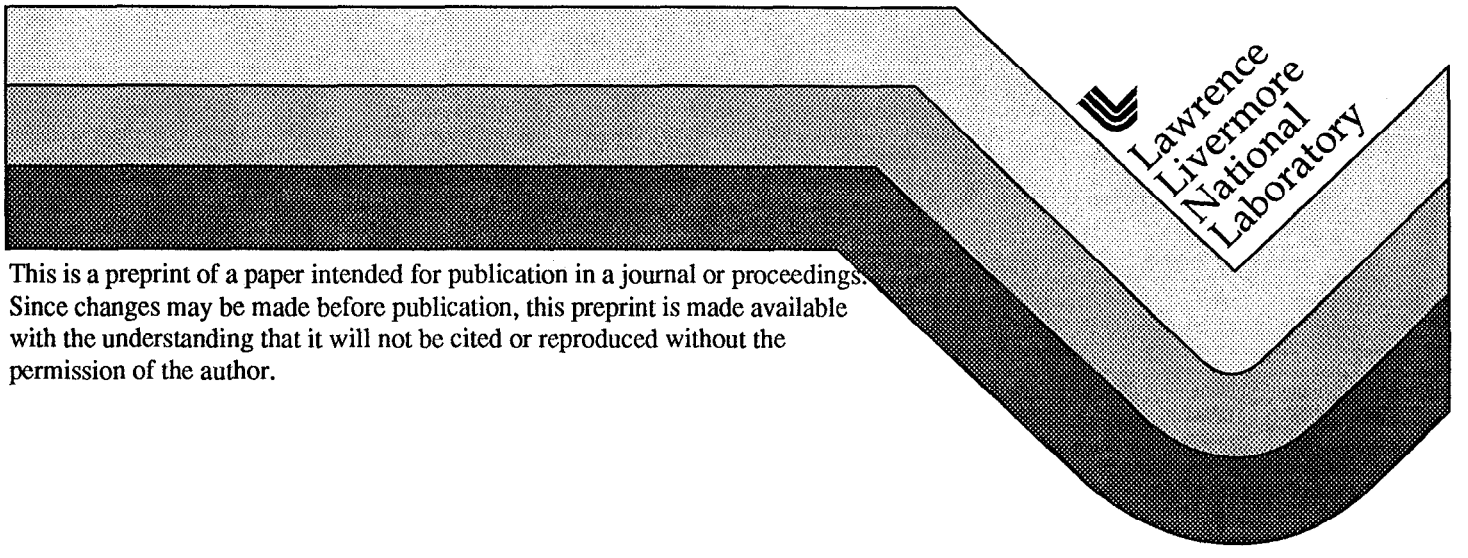

7th International Conference on Nuclear Engineering
Tokyo, Japan, April 19-23, 1999
ICONE-7048

STRESS CORROSION CRACKING OF Ni-BASE AND Ti ALLOYS UNDER CONTROLLED POTENTIAL

Ajit K. Roy
Framatome Cogema Fuels
c/o LLNL (On Assignment)
7000 East Ave, M/S L-369, Livermore, CA 94550, USA
Phone: 925-424-4829, Fax: 925-422-2118
E-mail: roy4@llnl.gov

John C. Estill
Steven R. Gordon, and
Lawrence F. Logoteta
Lawrence Livermore National Laboratory

ABSTRACT

Susceptibility to stress corrosion cracking (SCC) of alloy C-22 and Ti Gr-12, two candidate alloys for the inner-container of the multi-barrier nuclear waste package, was evaluated by using the slow-strain-rate (SSR) test technique in a deaerated acidic brine (pH $\approx$ 2.70) at 90°C. The strain rate used was 3.3×10^{-6} sec^{-1}. Prior to being tested in the acidic brine, specimens of each alloy were pulled inside the test chamber in the dry condition at room temperature (RT). Then specimens were exposed to the test solution while being strained under different controlled electrochemical potentials. The magnitude of the controlled potential was selected based on the corrosion potential measured in the test solution prior to straining of the specimen. Results indicate that, for Ti Gr-12, the times to failure were significantly shorter compared to those for alloy C-22. Furthermore, Ti Gr-12 showed reduced ductility in terms of percent reduction in area and true fracture stress, as the controlled potential became more cathodic. Results also indicate that the time-to-failure and percent elongation reached the minimum values when Ti Gr-12 was tested under impressed potential of −1162 mV. Finally, metallographic examination was performed to evaluate the primary fracture, and the secondary cracking, if any, along the gage section of the broken tensile specimen.

Keywords: Stress corrosion cracking, slow-strain-rate test, nickel-base alloy, titanium alloy, and controlled electrochemical potential.

1 INTRODUCTION

The waste package design for nuclear spent fuel and defense high-level waste, that is being considered for viability assessment for the potential underground repository at Yucca Mountain, will consist of two layers of metal barriers. The outer cylindrical barrier, made of corrosion-allowance material, will be thicker than the inner-barrier, which will be fabricated from corrosion-resistant material. The thick corrosion-allowance outer-barrier is being designed to

degrade at a very low rate resulting from the potential repository environment, while providing galvanic protection to the thinner corrosion-resistant inner-barrier. The precise method of fabricating these waste packages has not yet been finalized. Regardless of the fabrication technique, some form of welding of the container materials will be involved in producing cylindrical packages of large diameters. This welding could generate enough residual stresses causing the waste package materials to become susceptible to SCC as they come in contact with the repository environment. This paper presents the results of SCC tests of two candidate inner-container alloys exposed to an aqueous environment similar to that of the potential underground repository.

2 MATERIALS AND EXPERIMENTAL PROCEDURE

Materials tested include nickel-chromium-molybdenum (Ni-Cr-Mo) alloy C-22 and titanium (Ti)-base alloy Ti Gr-12. The chemical compositions and room-temperature mechanical properties of these alloys are given in Tables 1 and 2, respectively. The tensile specimens (7.25 inch long and 0.437 inch diameter with gage length and gage diameter of 1.0 inch and 0.100 inch, respectively) were machined from the mill-annealed plate materials in the longitudinal direction by a qualified vendor. No additional thermal treatments were given to these specimens prior to their testing.

The specimens were tested in a custom-made chamber made of polyvinylidene fluoride, and were vertically strained using an Instron Servohydraulic testing machine. A strain rate of 3.3×10^{-6} sec^{-1} was used in all experiments. The environment used for evaluating the susceptibility to SCC was a 90°C deaerated acidic brine (pH $\approx$ 2.70) containing 5 weight percent (wt%) NaCl. The selection of the acidic brine as test environment was based on the results of a recent SCC study[1] using the precracked double-cantilever-beam specimen, which showed crack growth in both alloy C-22 and Ti Gr-12 in a similar environment. Prior to being tested in the acidic brine, specimens of each alloy were pulled inside the test chamber in the dry condition at ambient temperature to establish a baseline. Specimens were then exposed to the acidic brine while being strained under different controlled electrochemical potentials (E_{cont}). The magnitude of E_{cont} was selected based on the stable open circuit or corrosion potential (E_{corr}), measured in the test solution prior to straining of the specimen. Ag/AgCl was used as the reference electrode in all SCC tests. Duplicate specimens of each material were tested under each experimental condition. The test setup is shown in Figure 1.

The load versus displacement curve for each specimen was recorded. The final gage length and gage diameter of the broken tensile specimen were measured. Ductility parameters such as the percent elongation (%El) and percent reduction in area (%RA) were calculated from the initial and final gage length and gage diameter, respectively. The maximum load prior to the failure of the test specimen was determined from the load versus displacement curve. The true fracture stress (σ_f) of the broken specimen was then calculated using this maximum load and the final cross sectional area at the gage section. The total time to failure (TTF) was determined from the change in gage length of the test specimen and the strain rate used.

Both broken halves of the test specimen were examined by optical microscopy to determine the extent of damage along the gage section. A section of the broken half showing the maximum damage was metallographically mounted and polished. A few selected specimens were also etched to determine the morphology of cracking. In addition, the primary fracture surfaces of some of the specimens were examined by optical microscopy.

At the time of writing of this paper, SCC testing of alloy C-22 specimens is still ongoing at different impressed cathodic potentials. Therefore, only limited data on alloy C-22 will be included in this paper. These data and overall results of SCC testing of Ti Gr-12 will be presented in the next section.

3 RESULTS AND DISCUSSION

For Ti Gr-12, cathodic (negative) potentials of 500, 1000 and 1200 mV with respect to the measured E_{corr} values were applied to the test specimens while being pulled. The average E_{cont} values corresponding to these applied potentials were –465, -970 and –1162 mV versus Ag/AgCl, respectively. An attempt was made to evaluate the effect of applied electrochemical potential on ductility parameters. These E_{cont} values and the average measured E_{corr} value (35 mV versus Ag/AgCl) of the test specimens that were tested without any externally applied potentials were plotted as functions of average σ_f, %RA, %El and TTF. The results indicate that the ductility of Ti Gr-12 in terms of both σ_f and %RA was gradually reduced with more cathodic E_{cont} values, as illustrated in Figures 2 and 3, respectively.

The effect of electrochemical potentiostatic polarization on %El and TTF for Ti Gr-12 are shown in Figures 4 and 5, respectively. It appears that both %El and TTF were slightly increased with applied cathodic potentials of –465 and –970 mV followed by a reduction of both parameters at an E_{cont} value of –1162 mV. Similarly, an evaluation of Figures 2 and 3 indicates that an application of –1162 mV to the Ti Gr-12 specimen produced the minimum σ_f and %RA values.

There are indications in the literature[2,3] that titanium and its alloys can absorb hydrogen when they are charged at cathodic potential or when they are galvanically coupled to more active metals and alloys, thus becoming cathodes. Hydrides can be formed in titanium alloys when the hydrogen absorption reaches a critical level. These hydrides, which are known to be brittle, can adversely influence the physical properties including all ductility parameters evaluated in this investigation. The detrimental effect of cathodic applied potentials in enhancing the hydrogen-induced embrittlement or hydrogen embrittlement (HE) of Ti Gr-3 (an α type titanium alloy) in 70°C acidic brine (6 wt% NaCl) has been reported by Wang et. al.[4] The formation of thicker hydride layers at more cathodic applied potentials has been attributed to the increased susceptibility to HE in their study.

The effect of hydrogen charging on the mechanical behavior of Ti-6Al-4V (an α-β type titanium alloy) has been investigated by Gu and Hardie.[5] They showed that the ductility of this alloy was drastically reduced when the hydrogen content exceeded a critical value of 2000 ppm. Their results suggest that Ti-6Al-4V may undergo HE at such hydrogen level. No attempt has yet been made to analyze the hydrogen content or the thickness of hydride layer formed along the gage section of the cathodically polarized Ti Gr-12 (a near-α type titanium alloy) tensile specimens used in this study. However, the use of forward recoil technique is being planned for hydrogen analysis involving the present and future test specimens.

The results of metallographic evaluation of broken Ti Gr-12 test specimens indicate that this alloy became susceptible to secondary cracking along the gage section while exposed to the test environment irrespective of the magnitude of E_{cont} values. However, no systematic correlation of

the measured deepest secondary crack length to the E_{cont} value could be made from this analysis. The nature of secondary cracking of Ti Gr-12 is shown in Figures 6 and 7. It appears that the cracking was transgranular in nature, as illustrated in the etched micrograph (Figure 6) for the specimen potentiostatically polarized at –465 mV versus Ag/AgCl. No attempt has yet been made to perform a fractographic evaluation of the primary failure of the broken specimen by scanning electron microscopy. However, a preliminary examination by optical microscopy revealed the characteristics of a brittle fracture resulting from the synergistic influence of applied stress and the environment used.

Initiation of SCC of titanium alloys in aqueous environments has been attributed[6,7] to planar slip and formation of wide slip steps that rupture the protective surface oxide film. Unless rapid repassivation of the surface film occurs, an active trench may be formed due to localized anodic dissolution at the metal surface. This active trench, if sufficiently localized, can eventually initiate the stress corrosion crack growth. Two theories have been proposed[6,7] to account for SCC propagation of titanium alloys in susceptible aqueous media. One theory[6,7] is based on anodic dissolution of metal surface at highly localized areas of stress concentration such as the crack tip, which can aid in crack propagation into the metal by the applied tensile stress.

The other prominent mechanism[6,7] is centered on the HE phenomenon that may possibly account for the cracking of Ti Gr-12 studied in this investigation. This mechanism postulates that hydrogen absorption can result from localized anodic dissolution in a hydrogen-containing aqueous solution, and generation of film-free surfaces within the advancing crack. Absorbed hydrogen may then migrate and concentrate in the vicinity of the crack tip due to the existing tensile stress gradients. Localized HE of the metal ahead of the crack tip can subsequently aid in continued growth of cracking. This mechanism has been cited[6,7] to be prominent for α and α/β types of titanium alloys, where localized precipitation of brittle titanium hydrides ahead of the advancing crack could promote transgranular brittle failure.

The preliminary data on alloy C-22 indicate that, compared to Ti Gr-12, this alloy showed significantly improved ductility under similar experimental conditions. The change in testing environment from RT air to 90°C acidic brine (with and without applied potential) did not have any significant impact on the resultant ductility. Both %RA and %El were only slightly reduced due to straining of this alloy in an aggressive aqueous solution, as shown in Table 3. The magnitude of σ_f value for this alloy was much higher compared to that of Ti Gr-12. In addition, this material took much longer duration to produce final fracture at the gage section even though the strain rate was identical for both alloys. It is also important to mention that the failure times for alloy C-22 were almost identical (Table 3) suggesting that this alloy may not undergo SCC under experimental conditions tested so far.

An examination of the primary fracture face by optical microscopy revealed cup and cone fracture in all tested alloy C-22 specimens indicating a ductile failure. No secondary crack was detected along the gage section of these specimens by metallography.

4 SUMMARY AND CONCLUSIONS

Smooth tensile specimens were tested to evaluate the SCC behavior of alloy C-22 and Ti Gr-12 in a 90°C acidic brine with and without impressed cathodic potential at a strain rate of 3.3×10^{-6} sec^{-1}. A few tests were also performed inside the test chamber in the dry condition at RT.

The morphology and the extent of cracking in the test specimens were evaluated by optical microscopy. Both primary and secondary cracking were examined. The significant conclusions drawn from this investigation are summarized below.

- The ductility of Ti Gr-12 in terms of σ_f and %RA was gradually reduced with more cathodic E_{cont} values. Slight increase in %El and TTF were noticed at E_{cont} values of –465 and –970 mV (Ag/AgCl) followed by their reduction at an E_{cont} value of –1162 mV (Ag/AgCl).

- The secondary cracking along the gage section of all potentiostatically polarized Ti Gr-12 specimens was transgranular in nature, confirming observations by other investigators. The primary fracture face showed the characteristics of a brittle failure.

- The initiation and growth of cracking of Ti Gr-12 could be attributed to the HE phenomenon resulting from the absorption of hydrogen due to cathodic charging and localized precipitation of brittle titanium hydrides ahead of the advancing crack, thus promoting transgranular failure.

- Alloy C-22 was immune to SCC under environmental conditions used in a limited number of experiments performed so far.

ACKNOWLEDGMENTS

This work was performed under the auspices of the U.S. Department of Energy under contract number W-7405-ENG-48 at the Lawrence Livermore National Laboratory. The support of the Yucca Mountain Site Characterization Project is thankfully acknowledged.

Thanks and appreciation are also extended to Robert Kershaw and Dennis Fleming for their sincere assistance in metallography and computer plotting of experimental data, respectively.

REFERENCES

1. A. K. Roy, D. L. Fleming and B. Y. Lum, "Stress Corrosion Cracking of Fe-Ni-Cr-Mo, Ni-Cr-Mo and Ti Alloys in 90°C Acidic Brine," NACE Corrosion/98, Paper No. 157, San Diego, CA, March 22-27, 1998

2. R. W. Schutz and J. S. Grauman, "Determination of Cathodic Potential Limits for Prevention of Titanium Tube Hydride Embrittlement in Salt Water," NACE Corrosion/89, Paper No. 110, New Orleans, LA, April 17-21, 1989

3. H. Satoh, T. Fukuzuka, K. Shimogori and H. Tanabe, "Hydrogen Pickup by Titanium Held Cathodic in Seawater," 2nd Int. Cong. Hydrogen in Metals, Paper No. 6A1, Paris, France, June 6-11, 1977

4. Z. F. Wang, C. L. Briant and K. S. Kumar, "Hydrogen Embrittlement of Grade 2 and Grade 3 Titanium in 6% Sodium Chloride Solution," Corrosion Vol. 54, No. 7, pp. 553-560, 1998

5. J. Gu and D. Hardie, "Effect of hydrogen on structure and slow strain rate embrittlement of mill annealed Ti6Al4V," Materials Science and Technology (UK), Vol. 12, No. 10, pp. 802-807, 1996

6. R.J.H. Wanhill, "Aqueous Stress Corrosion in Titanium Alloys," Br. Corros. J., Vol. 10, No. 2, pp. 69-78, 1975

7. J. Brettle, "Stress Corrosion of Titanium and Its Alloys in Aqueous Chloride Environments," Met. Mater., pp. 442-451, October 1972

Table 1

Chemical Composition of Materials Tested (wt%)

Material	Lot #	C	Mn	P	S	Si	Cr	Ni	Mo	Fe	Ti	Al	Cu	Other
Alloy C-22	M830	0.013	0.21	0.007	<0.005	0.01	21.61	Bal	13.19	4.57	---	---	---	W: 3.08 V: 0.14 Co: 1.76
Ti Gr-12	N242	0.007	---	---	---	---	---	0.93	0.31	0.18	Bal	---	---	H: 0.0051 O: 0.12 N: 0.008

Table 2

Room Temperature Mechanical Properties

Material	Lot #	YS (ksi)	UTS (ksi)	%El	%RA	Hardness
Alloy C-22	M830	54.50	117	60	N/A	N/A
Ti Gr-12	N242	56.50	80.70	18	N/A	N/A

N/A: Not Available

Table 3

SSR Test Results for Alloy C-22 Specimens

Environment	%El	%RA	σ_f (ksi)	TTF (h)
Air	57.2	80.3	587	48.1
5 wt% NaCl, pH ≈ 2.70, 90°C, E_{cont}: -131 mV (Ag/AgCl)	55.8	70.6	328	46.9
5 wt% NaCl, pH ≈ 2.70, 90°C, E_{cont}: -631 mV (Ag/AgCl)	55.8	67.7	332	47.0

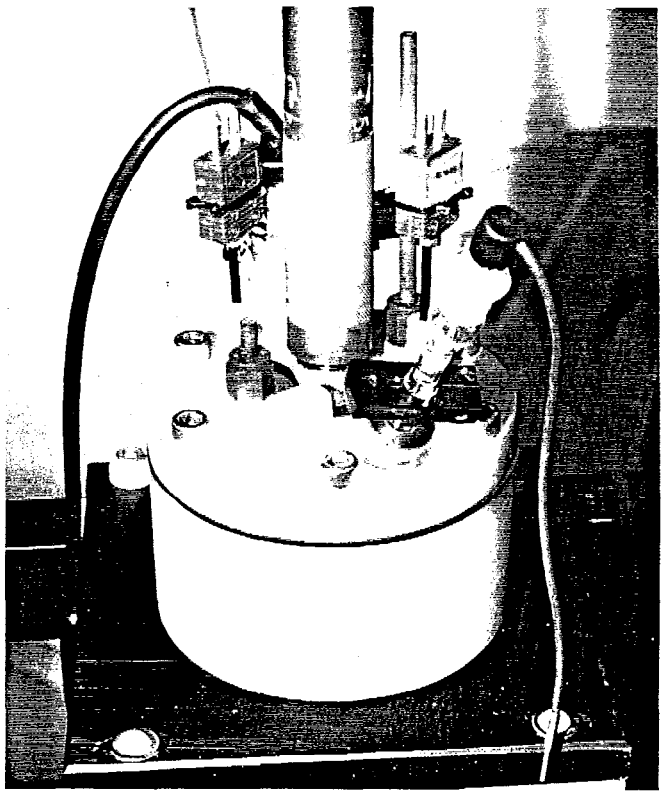

Figure 1. Experimental Setup

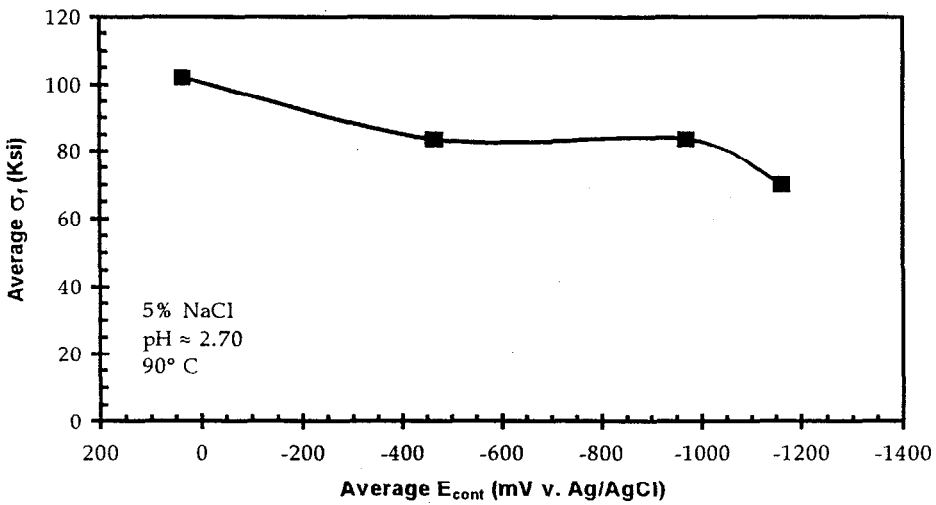

Figure 2. σ_f versus E_{cont} for Ti Gr-12

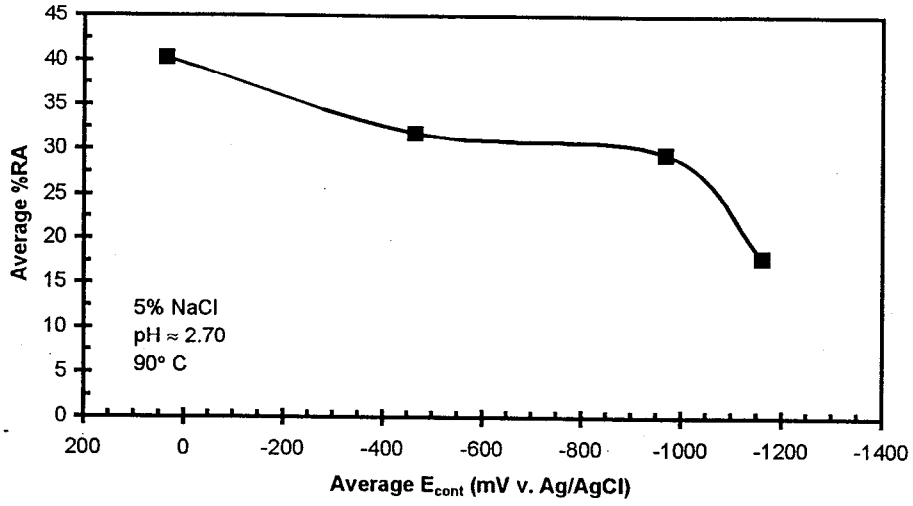

Figure 3. %RA versus E_{cont} for Ti Gr-12

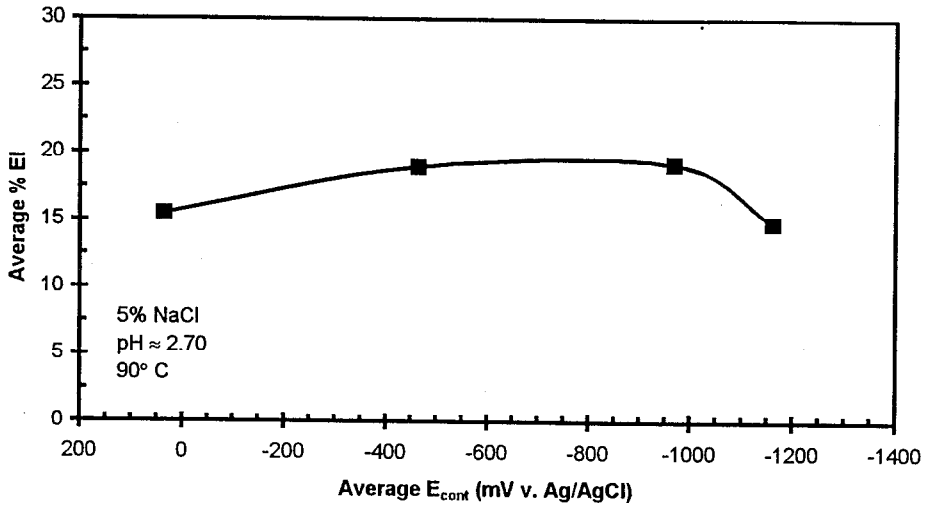

Figure 4. %El versus E_{cont} for Ti Gr-12

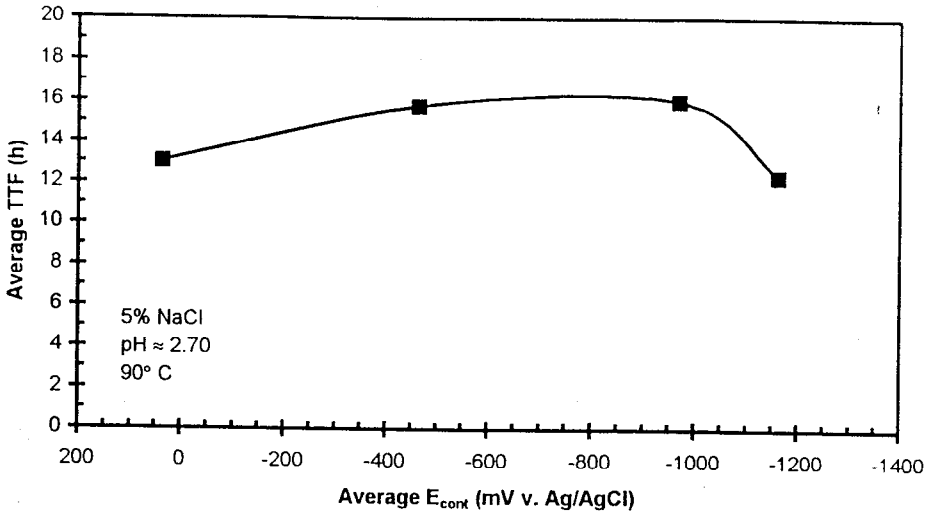

Figure 5. TTF versus E_{cont} for Ti Gr-12

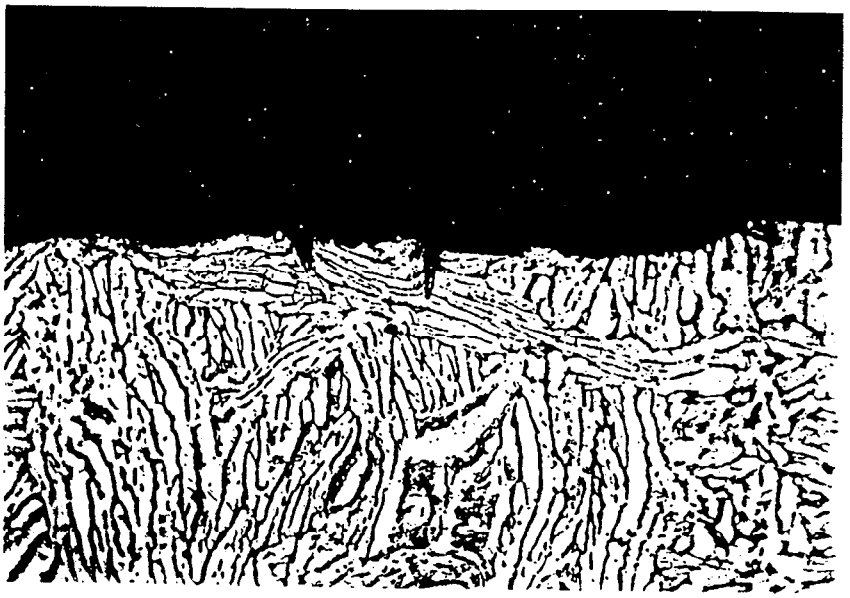

Figure 6. Secondary Cracking of Ti Gr-12 at an E_{cont} Value of –465 mV (Ag/AgCl). Etchant: 3% HF+6% HNO_3+Water, 500X

Figure 7. Secondary Cracking of Ti Gr-12 at an E_{cont} Value of –970 mV (Ag/AgCl). 500X